Arab J. Nucl. Sci. Appl., Vol. 55, 4, 1-15 (2022)

ISSN 1110-0451

Arab Journal of Nuclear Sciences and Applications

Web site: ajnsa.journals.ekb.eg

(E S N S A)

Dispersion of Natural Radionuclides and Radiological Characterization in Sedimentary Rocks at West of Gabal Adediya, Sinai, Egypt

Aya M. Zaghloul[a,*], Hosnia M. Abu-Zeid[a], Ibrahim E. El Aassy[b], Shadia M. Talaat[a], Thanaa M. Abd El Maksoud[a]

[(a)]Physics Department, Faculty of Women for Arts, Science and Education, Ain Shams University, Cairo11757, Egypt
[(b)]Nuclear Materials Authority, El-Maadi, Cairo530, Egypt

ARTICLE INFO

Article history:

Received: 15th Mar. 2022
Accepted: 14th June 2022

Keywords:

Natural Radioactivity;
Hazard Parameters;
Sedimentary Rocks;
West Gabal Adediya;
Sinai, Egypt.

ABSTRACT

The main natural radionuclides U-238, Th-232, U-235, and the members of their decay chain were studied in detail. P-type HPGe detector was used for specific activity concentration measurements. The present work stresses on the distribution of these natural radionuclides in forty-five sedimentary rock samples collected from west Gabal Adediya, southwestern Sinai, Egypt. The average activity concentrations for ^{238}U, ^{232}Th, and ^{40}K ranged between 104.38 ± 42.16 Bq/kg and 4507.41 ± 202.96 Bq/kg, 9.97 ± 2.2Bq/kg and 143.83 ± 14.53 , and 60.02 ± 3.78 Bq/kg and 1567.34 ± 9.11 Bq/kg with an average value of 1016.31 ± 83.87 Bq/kg, 87.39 ± 10.10, and 804.53 ± 7.32 Bq/kg respectively. The obtained values were higher than the recommended values. Radiological hazard parameters were estimated based on the activity concentrations of ^{226}Ra, ^{232}Th, and ^{40}K to find out any radiation hazard associated with these sediments. The radiological hazard parameters such as: absorbed gamma dose rates in air(D_{air}), annual effective dose equivalent ($AEDE$), external hazard index (H_{ex}) internal hazard index (H_{in}), the annual gonad equivalent dose ($AGED$), and excess lifetime cancer risk ($ELCR$), were calculated and compared with the internationally approved values and the recommended safety limits.

1. INTRODUCTION

Natural ionizing radiation is an unavoidable component of life. Every day, humans are exposed to natural background radiation emitted by the earth, building materials, air, food, outer space, and even substances within their own bodies. Gamma radiation emitted by primordial radionuclides and their products is one of the primary external sources of radiation exposure for human. A region's geological background and soil type determine terrestrial radioactivity and the resulting external gamma radiation exposure. Rocks and soils are two parameters that have strong influence on the dose distribution from natural terrestrial gamma radiation [1].

Gamma radiation emitted by potassium-40 naturally occurring radioactive materials and radionuclides from the ^{238}U and ^{232}Th series and their progenies(also known as terrestrial background radiation), which exist at detectable levels in all ground rock formation, is the primary external source of ionizing radiation to the midum [2].

The measurement of gamma radiation dose from natural sources is critical as the natural radiation is the primary contributor to global non-internal dose. The concentrations of radionuclide activity in the ecosystem differ with geologic formation; radionuclides in rocks are easily mobilized into the environment by both natural and anthropogenic activities [3].

Terrestrial and extraterrestrial radiations are present in the environment. As a result, primary radioactivity data collection and the derived radiological related parameters are critical aspects in terms of public

Corresponding author: aya.mohamed@women.asu.edu.eg
DOI: 10.21608/ajnsa.2022.129504.1566

awareness and environmental safety. The natural radioactivity found in soil, rock, sand, and other environmental materials significantly contributes to the total dose received by the living system [4].

The most commonly used analytical technique for estimating ^{238}U, ^{232}Th, and ^{40}K in various environmental samples is gamma-ray spectrometry. External contaminants, such as radionuclides, trace elements, or organic compounds, that enter a soil cell through wet or dry precipitation, behave differently in each soil type depending on absorption properties, texture, density, humidity, and other influences. The external gamma dose rate estimated is raising public awareness about radiation and providing important information about radiological protection [4].

The aim of the prestent study is the measurement of radioactive components for ^{235}U, ^{238}U,^{226}Ra, ^{232}Th, and ^{40}K in sedimentary rock samples collected from west Gabal Adediya by using a gamma ray spectrometry (HPGe) detector, and also, to assess the radiological hazard parameters. The outcomes are compared to similar studies conducted in other countries as well as the global database reported by [5,6].

2. GEOLOGY OF THE STUDIED AREA

The Sinai Peninsula is situated in the northeastern part of Egypt covering an area of about 23000 miles square (61000 Km^2). The studied area (Fig. 1) is located in southwestern, Sinai between longitudes 33° 23' 00″ and 33° 23' 30″ and Latitudes 28° 58' 00″ and 28° 58' 30″ N.

The Um Bogma Formation unconformably overlies the Adediya Formation [7]. It varies in thickness from 43 meters at Wadi Nukhul to 2 meters at Gabal Ghorabi.

The studied samples are belonging to the Um Bogma Formation of the early Carboniferous age (≃360 Ma). This Formation (Fig. 2) is classified into three members named from the older to the younger as follows:

a. The lower member: Shale ore-sandy dolomite beds with thin shale intercalations. The word ore means that, it contains one or more valuable minerals such as manganese- iron ore [8,9]. It is about 2-3 *m* in thickness in the studied area.

b. The middle member (4*m* thick) consists of shale, marl, and sandy dolostone and represents the most important member from the radioactivity point of view [10].

c. The upper member (3m thick*)* consists of sandy dolostone, jointed and fractured [11].

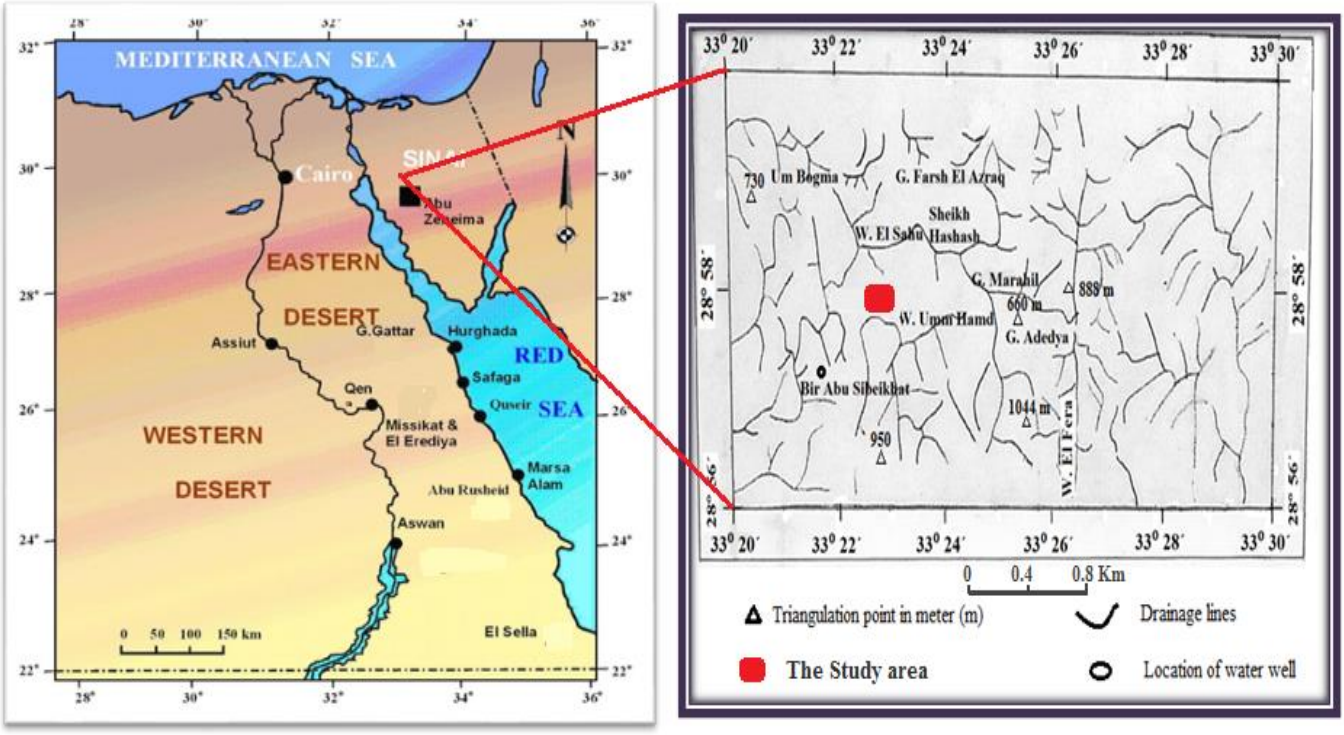

Fig. (1): Drainage map showing the studied area

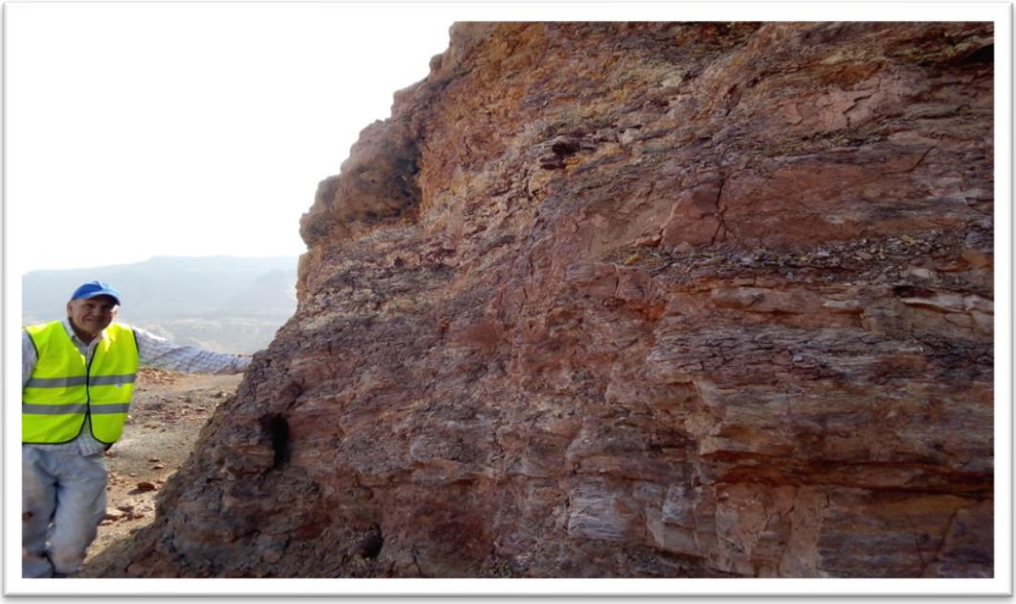

Fig. (2): West Gabal Adediya

2.1 Sampling and Sample Preparation

Forty-five sedimentary samples were collected from three different members (upper, middle and lower) of the studied area. The samples have different lithology, namely, siltstone, claystone, dolostone, shale, and dolomite. Twenty-three samples were crushed using a crushing machine at the laboratory of the Nuclear and Radiation Safety Research Center and the remaining twenty-two samples were crushed at the laboratory of Al-Azhar University, Faculty of Engineering. To avoid cross contamination of the samples, the machine was thoroughly cleaned after each pulverizing process. Each sample was crushed and grounded to about 63 mesh and then quartered to get representative samples for carrying out the experimental measurements and analyses.

These samples were packed in a cylindrical plastic container of constant volume (200 ml) to ensure geometric homogeneity around the detector, and the respective net masses were measured and recorded using a highly sensitive digital weighing balance with a percent of 0.01% correctness. The cylindrical plastic container was then sealed with plastic tape to prevent airborne radionuclides from escaping and left for at least four weeks to establish secular equilibrium.

2.2 Gamma-Ray Spectrometry

The gamma ray spectrometry was carried out using a high purity germanium (HPGe) detector, coaxial, p-type with a relative efficiency of about 50% of the 3″x3″ NaI(Tl) crystal efficiency. The full width at half maximum (FWHM) at 122 keV, Co-57 is 0.8 keV, and at 1332 keV, Co-60 is 1.9 keV. A 10 cm thick lead cylinder shield, internally coated with 2 mm thick copper foil, isolates the detector from background radiation. The gamma detector was chilled with liquid nitrogen at 77 K to reduce leakage current and thermal disturbance. The detector is connected to a multi-channel analyzer (MCA) card installed in a personal computer (PC) and is matched to conventional electronics. The data was collected and analyzed using the software program MAESTRO -32. The detection system's energy and efficiency calibrations are accomplished using a set (RG-set) of high-quality certified reference sources [12]. The HPGe detector was calibrated for efficiency using the reference material RGU-1 from IAEA. The certified activity of uranium is 4940 Bq/kg. Calibrations were performed by placing the reference source in the same position as the samples when determining their gamma-ray spectra. The minimum detectable activity (MDA) for radionuclides ^{235}U, ^{238}U, ^{232}Th, and ^{40}K are 0.5 Bq/kg, 4.07 Bq/kg, 0.56 Bq/kg, and 4.33 Bq/kg respectively.

The 1460.8 keV photopeak was used to measure the concentration of ^{40}K. Under the conditions of secular equilibrium, the uranium-235 activity was measured by its gamma ray photopeaks: 143.8, 163.4 and 205.3 keV [13]. The counting rate under the 63 keVpeak, was measured from the following equation [14]:

$$C\,(63) = C\left(^{234}Th\,, 63.3\right) + C\left(^{232}Th\,, 63.9\right) \qquad \textbf{(1)}$$

; where $C\left(\,^{A}X, E_{\gamma}\right)$ is the counting rate occurring from a gamma ray of energy E_{γ}, emitted by the nuclide ^{A}X. Equation (2) was used to calculate the contribution at 63.9 keV:

$$C\left(^{232}Th, 63.9\right) = \frac{\varepsilon(63.9)\times I\left(^{232}Th, 63.9\right)}{\varepsilon(338.32)\times I\left(^{228}Ac, 338.32\right)} \times C\left(^{228}Ac, 338.32\right) \quad \textbf{(2)}$$

where $I\left(^{A}X, E_\gamma\right)$ and $\varepsilon\left(E_\gamma\right)$ are the emission probability and detection efficiency for the E_γ keV gamma-ray.

^{238}U activity was determined indirectly from two gamma rays emitted by its daughter product (^{234m}Pa) whose activities are determined from the 1510.1 and 1001 keV photopeaks [15]. The counting rate under the 1510 keV peak, was given in equation (3):

$$C(1510) = C(^{214}Bi, 1509.2) + C(^{234m}Pa, 1510.1) \quad \textbf{(3)}$$

The contribution at 1510.1 keV may be isolated by using the clean $1001\,keV$ gamma ray of ^{234m}Pa by substituting in equation (4) [14]:

$$C(^{234m}Pa, 1510.1) = \frac{\varepsilon(1510.1)\times I(^{234m}Pa, 1510.1)}{\varepsilon(1001)\times I(^{234m}Pa, 1001)} \times C\left(^{234m}Pa, 1001\right) \quad (\textbf{4})$$

The 295.1 and 352 keV two gamma photopeaks were used to determine the activity concentration of ^{214}Pb, whereas the activity concentration of ^{214}Bi was established using the 609.3, 1120.3 and 1764.5 keV gamma photopeaks [13]. The specific activity of radium-226 was determined using the 186.1 keV from its own gamma-ray. The peak at 186 keV was used in the present study, considering that [14]:

$$C\ (186) = C\left(^{235}U\ , 185.7\right) + C(^{226}Ra\ , 186.1\big) \quad (\textbf{5})$$

The contribution at 186.1 keV can be isolated by substituting in equation (6) using the clean gamma ray 295.1 keV of ^{214}Pb [14]:

$$C(^{226}Ra, 186.1) = \frac{\varepsilon\ (186.1)\times I(^{226}Ra, 186.1)}{\varepsilon\ (295.1)\times I(^{214}Pb, 295.1)} \times C\left(^{214}Pb, 295.1\right) \quad (\textbf{6})$$

1. RESULTS AND DISCUSSION

3.1. Radioactivity Concentration

Forty-five sedimentary samples from west Gabal Adediya area were measured radiometrically using HPGe gamma ray spectrometry. Table (1) shows the specific average activity concentrations (Bq/kg) of ^{238}U, ^{235}U and their ratios $^{238}U/^{235}U$ in the studied area. The forty-five samples were collected from three members: upper (6 samples), middle (34 samples) and lower (5 samples).

At the upper member, Table (1) shows that the average activity concentration of U-238 ranged between 221.78 ± 40.58 Bq/kg and 354.27 ± 52.70 Bq/kg with an average value of 298.88 ± 47.22 Bq/kg. ^{235}U ranged between 10.22±1.01Bq/kg and 16.22±1.30 Bq/kg with an average value of 13.82±1.19 Bq/kg.

At the middle member (top meter), the average activity concentration of U-238 ranged between 162.36 ± 46.35 Bq/kg and 4507.41± 202.96 Bq/kg with an average value of 1713.44±108.54 Bq/kg. The activity concentration of ^{235}U ranged between 7.50± 1.22 Bq/kg and 205.85± 5.25 Bq/kg with an average value of 77.79± 3.01 Bq/kg.

At the middle member (middle meter), the activity concentration of ^{238}U ranged between 192.56 ± 31.05 Bq/kg and 1911.00 ± 104.83 Bq/kg with an average value of 895.70 ± 80.02 Bq/kg. While the activity concentration of ^{235}U ranged between 9.04 ± 1.00 Bq/kg and 87.87 ± 3.02 Bq/kg with an average value of 41.17 ± 2.31 Bq/kg.

At the base meter (middle member), the average activity concentration of ^{238}U ranged between 474.12 ± 45.97 Bq/kg and 2022.19 ± 154.95 Bq/kg with an average value of 994.63 ± 95.91 Bq/kg. The activity concentration of ^{235}U ranged between 21.87 ± 1.75 Bq/kg and 93.20 ± 4.00 Bq/kg with an average 45.80 ± 2.48 Bq/kg.

At the lower member, the average activity concentration of ^{238}U ranged between 104.38± 42.16 Bq/kg and 416.92 ± 61.07 Bq/kg with an average value of 249.39 ± 48.74 Bq/kg. The activity concentration of ^{235}U ranged between 4.83 ± 0.88 Bq/kg and 19.21 ± 2.24 Bq/kg with an average 11.55±1.39 Bq/kg.

The average activity concentrations (Bq/kg) of ^{226}Ra, ^{232}Th and ^{40}K for all different sedimentary samples corresponding to their lithology collected from the studied area are given in Table (2). The average activity concentrations of ^{226}Ra, ^{232}Th and ^{40}K for siltstone are 1480.81±10.61 Bq/kg, 95.45±10.84 Bq/kg and 875.20±7.84 Bq/kg, respectively.

For claystone the average activity concentrations of ^{226}Ra, ^{232}Th and ^{40}K are 645.85±7.86 Bq/kg, 104.83±11.61 Bq/kg and 1018.28±7.84 Bq/kg, respectively. While for shale, the average activity concentration of ^{226}Ra, ^{232}Th and ^{40}K are 208.74±5.20 Bq/kg, 98.43±11.13 Bq/kg and 818.03±7.03 Bq/kg, respectively. For dolostone, the average activity concentrations of ^{226}Ra, ^{232}Th and ^{40}K are 229.71±4.65 Bq/kg, 10.95±3.31 Bq/kg and 75.57±4.84 Bq/kg, respectively. As for dolomite, the average activity concentrations of ^{226}Ra, ^{232}Th and ^{40}K are 198.57±4.88 Bq/kg, 11.94±3.32 Bq/kg and 60.02±3.78 Bq/kg, respectively.

Table (1): The average activity concentrations (Bq/kg) of ^{238}U, ^{235}U and their ratios for the investigated area

Member	Lithology	Sample ID	^{234m}Pa (1001 keV)	^{234m}Pa (1510 keV)	^{238}U (Average)	^{235}U	$\frac{^{238}U}{^{235}U}$
Upper Member	Dolostone (Base)	U67	331.98 ± 11.32	331.23 ± 55.64	331.60 ± 33.48	15.35 ± 0.87	21.60
	Dolostone (Top)	U68	281.15 ± 18.85	280.37 ± 83.58	280.76 ± 51.22	13.05 ± 1.14	21.52
	Dolostone (Top)	U69	295.49 ± 19.34	294.73 ± 92.45	295.11 ± 55.90	13.72 ± 1.43	21.51
	Dolostone (Base)	U73	354.65 ± 19.91	353.89 ± 85.48	354.27 ± 52.70	16.22 ± 1.30	21.85
	Dolostone (Top)	U74	310.14 ± 16.73	309.37 ± 82.11	309.76 ± 49.42	14.34 ± 1.37	21.60
	Dolomite (Top)	U75	222.16 ± 15.78	221.40 ± 65.38	221.78 ± 40.58	10.22 ± 1.01	21.70
		Range	222.16 - 354.65	221.40 - 353.89	221.78 - 354.27	10.22 - 16.22	-
		Average	299.26 ± 16.99	298.50 ± 77.44	298.88 ± 47.22	13.82 ± 1.19	-
Middle Member (Top Meter)	Siltstone (East R.H)	U1	377.70 ± 20.59	376.72 ± 94.40	377.21 ± 57.49	17.21 ± 1.28	21.92
	Claystone (In Medium)	U2	613.92 ± 26.12	612.98 ± 124.50	613.45 ± 75.31	27.92 ± 2.14	21.98
	Siltstone	U3	174.03 ± 32.34	188.34 ± 87.04	181.19 ± 59.69	8.03 ± 1.57	22.55
	Shale (West L.H)	U4	193.53 ± 19.20	192.70 ± 66.75	193.12 ± 42.97	8.92 ± 1.35	21.64
	Siltstone (West L.H)	U5	4507.90 ± 66.00	4506.92 ± 339.92	4507.41 ± 202.96	205.85 ± 5.25	21.90
	Claystone (Top)	U6	2464.12 ± 39.17	2463.13 ± 216.55	2463.63 ± 127.86	115.60 ± 3.41	21.31
	Siltstone (Base)	U7	3362.56 ± 53.84	3361.67 ± 278.26	3362.11 ± 166.05	150.59 ± 4.83	22.33
	Siltstone (East R.H)	U18	327.63 ± 27.09	326.65 ± 96.40	327.14 ± 61.74	15.02 ± 1.42	21.78
	Claystone (In Medium)	U19	646.49 ± 28.25	645.56 ± 126.53	646.02 ± 77.39	29.68 ± 2.31	21.76
	Siltstone (West L.H)	U20	162.83 ± 22.50	161.90 ± 70.19	162.36 ± 46.35	7.50 ± 1.22	21.66
	Shale (West L.H)	U21	188.04 ± 19.58	187.21 ± 72.52	187.62 ± 46.05	8.65 ± 1.37	21.68
	Siltstone (West L.H)	U22	4507.37 ± 70.46	4506.40 ± 367.85	4506.88 ± 219.16	202.96 ± 5.88	22.21
	Claystone (Top)	U23	2568.20 ± 49.63	2567.23 ± 252.85	2567.72 ± 151.24	119.31 ± 4.34	21.52
	Siltstone (Base)	U24	3892.73 ± 64.74	3891.80 ± 305.88	3892.26 ± 185.31	171.81 ± 5.81	21.96
		Range	162.83-4507.90	161.90-4506.92	162.36-4507.41	7.50-205.85	-
		Average	1713.36 ± 38.54	1713.52 ± 178.55	1713.44 ± 108.54	77.79 ± 3.01	-

Continue, Table (1)

Member		Lithology	Sample ID	^{234m}Pa (1001 keV)	^{234m}Pa (1510 keV)	^{238}U (Average)	^{235}U	$\frac{^{238}U}{^{235}U}$
	(Middle Meter)	Shale (East R.H)	U8	293.31 ± 25.60	292.37 ± 98.11	292.84 ± 61.86	13.86 ± 1.43	21.14
		Claystone (In Medium)	U9	424.87 ± 25.48	423.93 ± 118.56	424.40 ± 72.02	19.57 ± 1.98	21.69
		Siltstone (In Medium)	U10	192.99 ± 11.72	192.12 ± 50.38	192.56 ± 31.05	9.04 ± 1.00	21.30
		Siltstone (West L.H)	U11	1614.53 ± 42.57	1613.60 ± 191.17	1614.06 ± 116.87	72.78 ± 3.61	22.18
		Siltstone (Top)	U12	1903.92 ± 28.80	1903.10 ± 143.12	1903.51 ± 85.96	85.58 ± 2.25	22.24
		Siltstone (Base)	U13	964.38 ± 34.62	963.35 ± 164.32	963.86 ± 99.47	44.04 ± 2.83	21.88
		Shale (East R.H)	U25	271.64 ± 26.19	270.70 ± 95.31	271.17 ± 60.75	12.57 ± 1.76	21.58
		Claystone (In Medium)	U26	317.02 ± 24.78	316.09 ± 102.25	316.56 ± 63.52	14.34 ± 1.63	22.08
		Claystone (In Medium)	U27	215.45 ± 18.00	214.57 ± 73.79	215.01 ± 45.90	10.10 ± 1.62	21.29
		Siltstone (West L.H)	U28	1747.60 ± 49.55	1746.68 ± 207.70	1747.14 ± 128.62	83.09 ± 4.16	21.03
		Siltstone (Top)	U29	1912.00 ± 35.77	1911.15 ± 173.88	1911.58 ± 104.83	87.87 ± 3.02	21.75
		Siltstone (Base)	U30	896.22 ± 31.27	895.21 ± 147.41	895.71 ± 89.34	41.19 ± 2.48	21.74
			Range	192.99 - 1912.00	192.12 - 1911.15	192.56 - 1911.58	9.04 - 87.87	-
			Average	896.16 ± 29.53	895.24 ± 130.50	895.70 ± 80.02	41.17 ± 2.31	-
	(Base Meter)	Siltstone (East R.H)	U14	474.63 ± 16.23	473.60 ± 75.70	474.12 ± 45.97	21.94 ± 1.29	21.61
		Siltstone (West L.H)	U15	2022.80 ± 52.99	2021.57 ± 256.91	2022.19 ± 154.95	93.20 ± 4.00	21.70
		Claystone (Top)	U16	749.75 ± 34.09	748.61 ± 168.37	749.18 ± 101.23	34.48 ± 2.34	21.73
		Siltstone (Base)	U17	898.73 ± 32.91	897.73 ± 163.36	898.23 ± 98.13	41.68 ± 2.39	21.55
		Claystone (East R.H)	U31	477.18 ± 27.30	476.19 ± 100.98	476.69 ± 64.14	21.87 ± 1.75	21.80
		Siltstone (West L.H)	U32	1619.19 ± 48.52	1618.00 ± 232.37	1618.59 ± 140.44	73.82 ± 4.14	21.93
		Claystone (Top)	U33	728.86 ± 32.48	727.70 ± 156.26	728.28 ± 94.37	33.55 ± 1.98	21.71
		Claystone (Base)	U34	990.24 ± 22.92	989.26 ± 113.15	989.75 ± 68.04	45.83 ± 1.95	21.59
			Range	474.63 - 2022.80	473.60 - 2021.57	474.12 - 2022.19	21.87 - 93.20	-
			Average	995.17 ± 33.43	994.08 ± 158.39	994.63 ± 95.91	45.80 ± 2.48	-
Lower Member		Claystone	U70	214.32 ± 19.74	213.43 ± 82.24	213.87 ± 50.99	9.97 ± 1.30	21.45
		Claystone	U71	406.42 ± 18.51	405.54 ± 87.42	405.98 ± 52.96	18.92 ± 1.50	21.46
		Siltstone	U72	99.29 ± 17.75	112.31 ± 55.34	105.80 ± 36.54	4.83 ± 0.88	21.90
		Claystone	U76	417.36 ± 23.99	416.48 ± 98.15	416.92 ± 61.07	19.21 ± 2.24	21.70
		Siltstone	U77	99.92 ± 23.94	108.83 ± 60.38	104.38 ± 42.16	4.84 ± 1.03	21.55
			Range	99.29 - 417.36	108.83 - 416.48	104.38 - 416.92	4.83 - 19.21	-
			Average	247.46 ± 20.79	251.32 ± 76.71	249.39 ± 48.74	11.55 ± 1.39	-

The average activity concentrations of ^{226}Ra, ^{232}Th, and ^{40}K for the studied sedimentary samples were given in Table (2). According to the obtained results for all studied samples, siltstone has a higher average activity concentration value for ^{238}U series, however claystone has higher values for ^{232}Th and ^{40}K. Variation among the radioactivity concentration for different locations has been observed, it may be due to geological condition[16].

Table (2): The average activity concentrations (Bq/kg) of ^{226}Ra, ^{232}Th and ^{40}K for all studied sedimentary samples according to their lithology

Lithology	Sample ID	^{226}Ra	^{232}Th	^{40}K
Siltstone	U1	311.00 ± 5.89	97.63 ± 10.74	1567.34 ± 9.11
	U3	142.97 ± 5.56	83.33 ± 12.09	565.57 ± 7.27
	U5	3598.46 ± 18.42	143.83 ± 14.53	1062.45 ± 9.55
	U7	3539.31 ± 18.12	109.51 ± 12.00	955.18 ± 8.69
	U18	283.22 ± 6.19	88.25 ± 10.86	1451.12 ± 9.38
	U20	124.99 ± 5.20	82.45 ± 9.89	555.94 ± 5.85
	U22	3538.52 ± 21.39	126.69 ± 14.68	1094.68 ± 10.98
	U24	3933.82 ± 18.59	123.73 ± 13.05	1023.39 ± 10.18
	U10	182.39 ± 3.37	103.03 ± 8.39	773.93 ± 4.89
	U11	2381.90 ± 13.78	73.76 ± 9.70	545.17 ± 6.93
	U12	1750.85 ± 8.62	97.16 ± 7.75	1022.75 ± 5.77
	U13	1024.14 ± 10.37	90.75 ± 11.71	864.25 ± 8.32
	U28	2589.92 ± 15.59	105.62 ± 12.12	542.60 ± 7.72
	U29	1915.48 ± 11.19	99.40 ± 9.47	1021.77 ± 7.05
	U30	961.40 ± 8.95	89.52 ± 10.87	831.99 ± 7.49
	U14	401.02 ± 4.67	122.84 ± 9.12	937.90 ± 5.39
	U15	1782.59 ± 14.09	125.75 ± 15.11	381.65 ± 7.53
	U17	818.75 ± 9.57	86.54 ± 11.69	1095.66 ± 9.26
	U32	1665.51 ± 14.30	123.25 ± 15.03	335.53 ± 7.69
	U72	76.39 ± 3.89	15.90 ± 4.32	*BLD**
	U77	74.29 ± 5.02	15.49 ± 4.42	*BLD*
	Range	74.29 - 3933.82	15.49 - 143.83	*BLD* - 1567.34
	Average	1480.81 ± 10.61	95.45 ± 10.84	875.20 ± 7.84
Claystone	U2	635.58 ± 7.35	97.78 ± 11.36	1475.63 ± 9.47
	U6	1645.85 ± 11.43	97.00 ± 10.22	1153.84 ± 7.97
	U19	642.81 ± 8.05	110.05 ± 11.99	1441.37 ± 7.00
	U23	1742.69 ± 13.79	92.90 ± 11.41	1121.23 ± 9.72
	U9	361.52 ± 7.71	105.62 ± 12.85	1293.02 ± 9.72
	U26	345.88 ± 7.35	100.41 ± 12.22	1228.51 ± 9.33
	U27	189.42 ± 5.74	119.64 ± 11.64	810.58 ± 6.59
	U16	623.91 ± 9.13	109.76 ± 14.50	1112.81 ± 10.21
	U31	391.97 ± 6.16	119.57 ± 11.59	931.13 ± 7.02
	U33	637.79 ± 8.73	103.73 ± 13.40	1147.81 ± 9.90
	U34	840.91 ± 6.62	104.33 ± 8.75	1073.55 ± 6.15
	U70	188.03 ± 4.93	117.07 ± 12.38	560.77 ± 6.16
	U71	414.75 ± 5.47	93.40 ± 9.61	448.39 ± 4.93
	U76	380.82 ± 7.57	96.32 ± 10.61	457.34 ± 5.55
	Range	189.42 - 1742.69	92.90- 119.64	448.39 - 1475.63
	Average	645.85 ± 7.86	104.83 ± 11.61	1018.28 ± 7.84

Continue, Table (2)

Lithology	*Sample ID*	^{226}Ra	^{232}Th	^{40}K
Shale	U4	152.73 ± 3.95	94.06 ± 9.77	697.83 ± 5.79
	U21	149.30 ± 4.54	94.26 ± 10.43	650.99 ± 6.07
	U8	270.09 ± 5.72	107.18 ± 12.46	996.23 ± 8.27
	U25	262.84 ± 6.57	98.23 ± 11.88	927.08 ± 7.98
	Range	149.30 - 270.09	94.06- 107.18	650.99 - 996.23
	Average	208.74 ± 5.20	98.43 ± 11.13	818.03 ± 7.03
Dolostone	U67	258.04 ± 3.23	9.97 ± 2.28	92.71 ± 1.88
	U68	208.42 ± 4.39	10.62 ± 3.51	64.64 ± 5.64
	U69	226.06 ± 5.07	11.99 ± 3.95	66.18 ± 8.19
	U73	242.38 ± 4.99	10.04 ± 3.23	84.72 ± 3.89
	U74	213.64 ± 5.56	12.16 ± 3.60	69.59 ± 4.59
	Range	208.42 - 258.04	9.97- 12.16	64.64 - 92.71
	Average	229.71 ± 4.65	10.95 ± 3.31	75.57 ± 4.84
Dolomite	U75	198.57 ± 4.88	11.94 ± 3.32	60.02 ± 3.78

BLD*: Below limit of Detection

For all the studied samples, ^{238}U average activity concentration ranged between 104.38 ± 42.16 Bq/kg and 4507.41 ± 202.96Bq/kg with an average value of 1016.31 ± 83.87 Bq/kg. ^{232}Th average activity concentration ranged between 9.97 ± 2.2Bq/kg and 143.83 ± 14.53 with an average value of 87.39 ± 10.10. While ^{40}K ranged between 60.02 ± 3.78 Bq/kg and 1567.34 ± 9.11 Bq/kg with an average value of 804.53 ± 7.32 Bq/kg.

The most contribution for the average activity concentrations of the radionuclides for the studied area (Fig. 3) are ^{238}U (35%) followed by ^{226}Ra (32%), ^{40}K(28%), ^{232}Th (3%) then ^{235}U (2%).

Figure 4 (a) shows that there is an equilibrium between ^{226}Ra *and* ^{238}U activity concentration for the middle member. Also, Fig. 4 (b, c, d) shows weak relations between the activity concentrations of (^{238}U and ^{232}Th), (^{238}U and ^{40}K), and (^{232}Th and ^{40}K), in the studied area respectively. This means that there is no significant correlation between ^{238}U and either ^{232}Th or ^{40}K, and also between ^{232}Th and ^{40}K, that may be indicating the pattern of significant geochemical weathering effect on these samples.

Table (3) shows a comparison between the average activity concentrations for ^{226}Ra, ^{232}Th, and ^{40}K in the studied area and other countries in the world. The present studied area has the highest average activity concentration for ^{226}Ra with a value of 940.46 Bq/kg, which is higher than that the world average value.

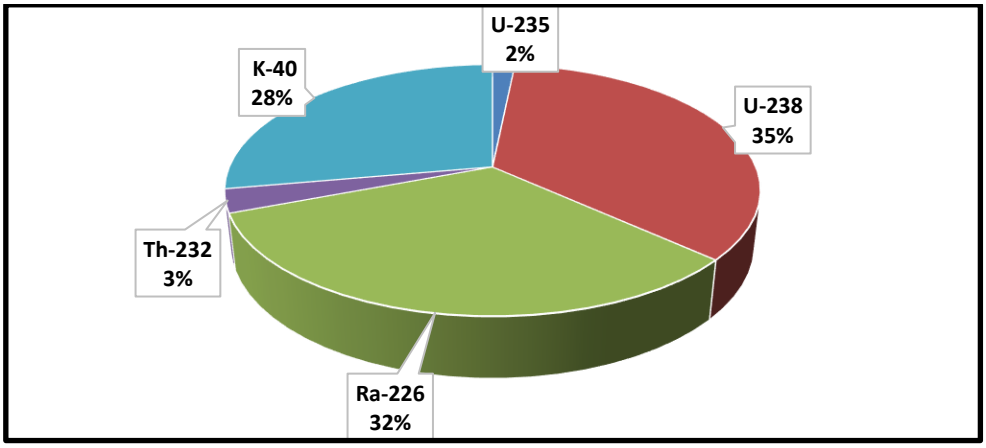

Fig. (3): Relative contribution of average activity concentrations for ^{238}U, ^{226}Ra, ^{235}U, ^{232}Th and ^{40}K for the studied area.

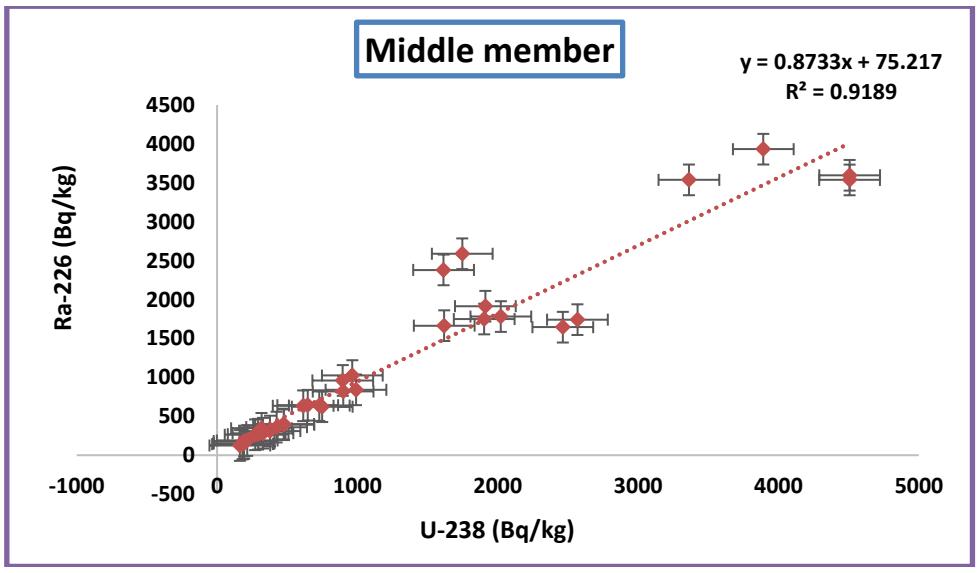

(a)

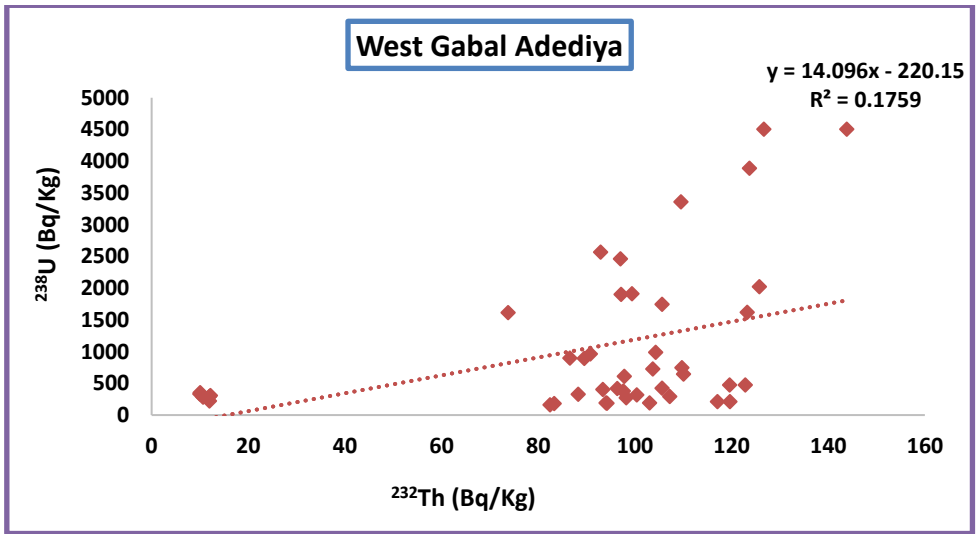

(b)

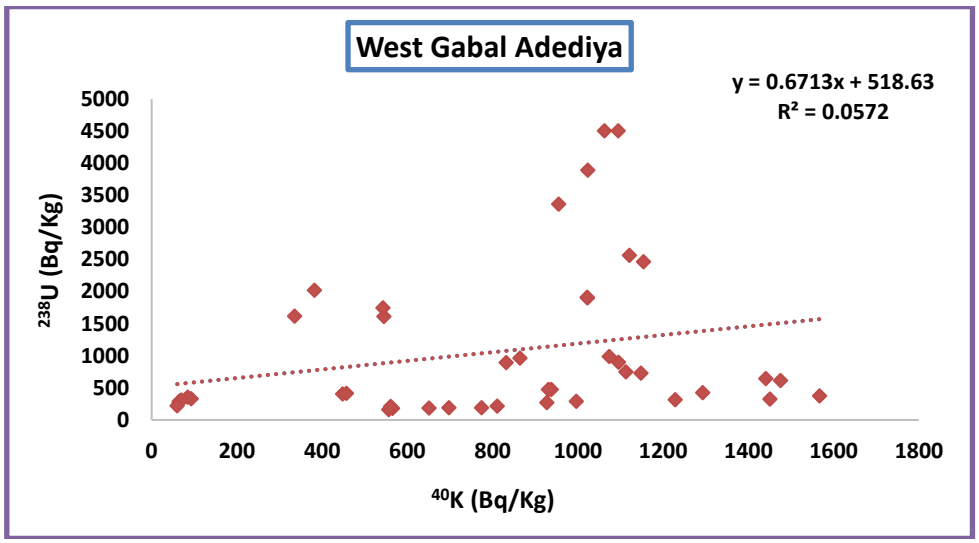

(c)

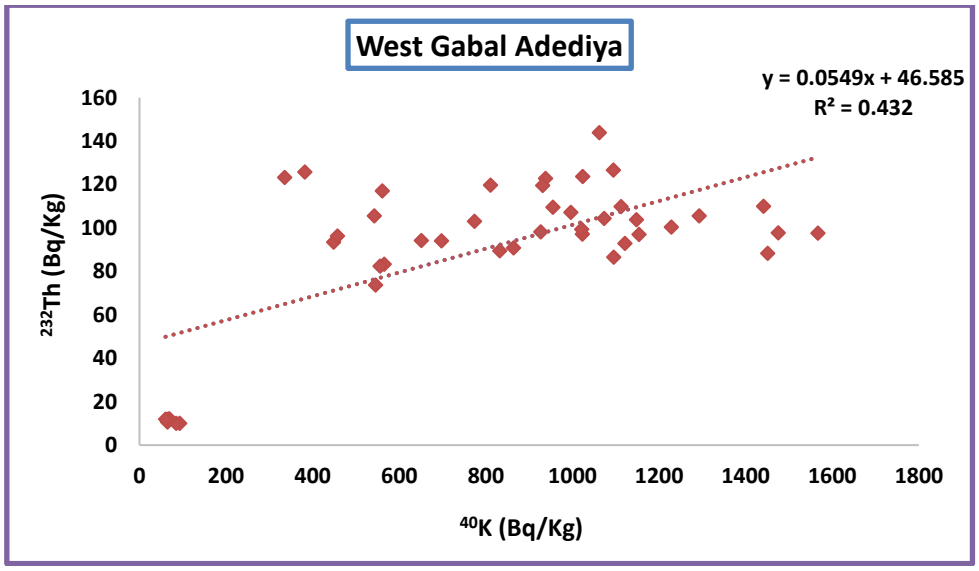

(d)

Fig. (4) (a, b, c, d): Correlations between the activity concentrations of (^{226}Ra and ^{238}U), (^{232}Th and ^{238}U), (^{40}K and ^{238}U), and (^{40}K and ^{232}Th) respectively.

Table (3): Comparison for ^{226}Ra, ^{232}Th and ^{40}K average activity concentration (Bq/kg) for west Gabal Adediya with other areas of the world

Country	^{226}Ra	^{232}Th	^{40}K	References
Sinai, Egypt	**940.46**	**87.39**	**804.53**	**Studied area**
Egypt	**215.43**	**131.26**	**822.76**	[17]
Turkey	**45.94**	**50.23**	**721.27**	[18]
Egypt	**30**	**20**	**430**	[19]
Nigeria	**25**	**77**	**710**	[20]
USA	**33.7**	**31.9**	**300**	[21]
West, Nigeria	**12.1**	**60.1**	**426.5**	[22]
China	**26**	**49**	**440**	[23]
The Worldwide Average	**32**	**45**	**412**	[5]

3.2. Radiological Risk Health Assessment

The aim of conducting a radiation risk assessment is to identify the measures needed to limit radiation exposures and address all relevant regulatory requirements. The threat assessment system has four distinct phases: hazard analysis, hazard classification, exposure assessment, and risk characterization. For forty-five sediment samples, radiological hazard indices were estimated and represented in Table (4).

3.2.1. Absorbed Dose Rate (D_{air})

The absorbed gamma dose rate in air one meter above the ground surface for a uniform distribution of radionuclides ^{226}Ra, ^{232}Th and ^{40}K was calculated using the provided guidelines. The conversion factors used to calculate the absorbed gamma dose rate in air (D_{air}) per unit activity concentration ($1Bq/kg$) are 0.462 for ^{226}Ra, 0.604 for ^{232}Th and 0.0417 for ^{40}K (equation (7))[24].

$$D_{air}(nGy\ h^{-1}) = 0.462\ A_{Ra} + 0.604\ A_{Th} + 0.0417\ A_K \quad (7)$$

where A_{Ra}, A_{Th}, and A_K are the activity concentrations of ^{226}Ra, ^{232}Th, and ^{40}K in the sediment samples, respectively. The mean absorbed dose rate value is 519.34 $nGyh^{-1}$ which is higher than the world limit with value 59 $nGyh^{-1}$.

3.2.2. Radium Activity Equivalent (Ra_{eq})

The gamma radiation hazards associated with materials containing ^{226}Ra, ^{232}Th, and ^{40}K were assessed using radium equivalent activity (Ra_{eq}). It is assumed that dose rates of 370 Bq/kg of ^{226}Ra, 259 Bq/kg of ^{232}Th, and 4810 Bq/kg of ^{40}K are comparable. Equation (8) gives the radium equivalent activity (Bq/kg) [1].

$$Ra_{eq} = A_{Ra} + 1.43A_{Th} + 0.07A_K \quad \textbf{(8)}$$

The radium activities equivalent for the middle member (Fig. 5) are higher than the world limit of 370 Bq/kg except four samples U3, U4, U20, and U21. The mean radium equivalent value at the middle member is 1387.42 Bq/kg which is higher than the permissible level (P.L). While at west Gabal Adediya, the average value of radium equivalent is 1119.24 Bq/kg which is exceed the permissible level.

3.2.3. Annual Effective Dose Equivalent ($AEDE_{outdoor}$ & $AEDE_{indoor}$)

These indices assess the risk of stochastic and deterministic effects in irradiated participants [24]. The AEDE (outdoor & indoor) were determined using the subsequent formulas:

$$AEDE_{(outdoor)}(mSv\ y^{-1}) = D\,(nGyh^{-1}) \times 8766h \times 0.2 \times 0.7(Sv\ Gy^{-1}) \times 10^{-6} \quad \textbf{(9)}$$

$$AEDE_{(Indoor)}(mSv\ y^{-1}) = D(nGyh^{-1}) \times 8766h \times 0.8 \times 0.7(SvGy^{-1}) \times 10^{-6} \quad \textbf{(10)}$$

The expected mean annual indoor effective dose from naturally occurring radionuclides (NORM) was 0.05 *mSv y^{-1}*, while outdoor was 0.7 *mSv y^{-1}* [25]. In the studied area, the average value of $AEDE_{outdoor}$ was 0.64 mSy^{-1} which is lower than the recommended value of 0.7 mSy^{-1}. While the average value of $AEDE_{indoor}$ was 2.55 mSy^{-1}, which is higher than the permissible value of 0.05 mSy^{-1}.

3.2.4. External (H_{ex}) and Internal (H_{in}) Hazard Indices

The major sources of radiation hazard threat to people are external and internal exposures. The external and internal radiological hazards posed by the soil in the studied area were quantified using equations (11) and (12) [26]**:**

$$H_{ex} = \frac{A_{Ra}}{370} + \frac{A_{Th}}{259} + \frac{A_K}{4810} \leq 1 \quad \textbf{(11)}$$

$$H_{in} = \frac{A_{Ra}}{185} + \frac{A_{Th}}{259} + \frac{A_K}{4810} \leq 1 \quad \textbf{(12)}$$

The mean H_{ex} and H_{in} values for all collected samples were 3.04 and 5.58, respectively, which exceed the recommended value1

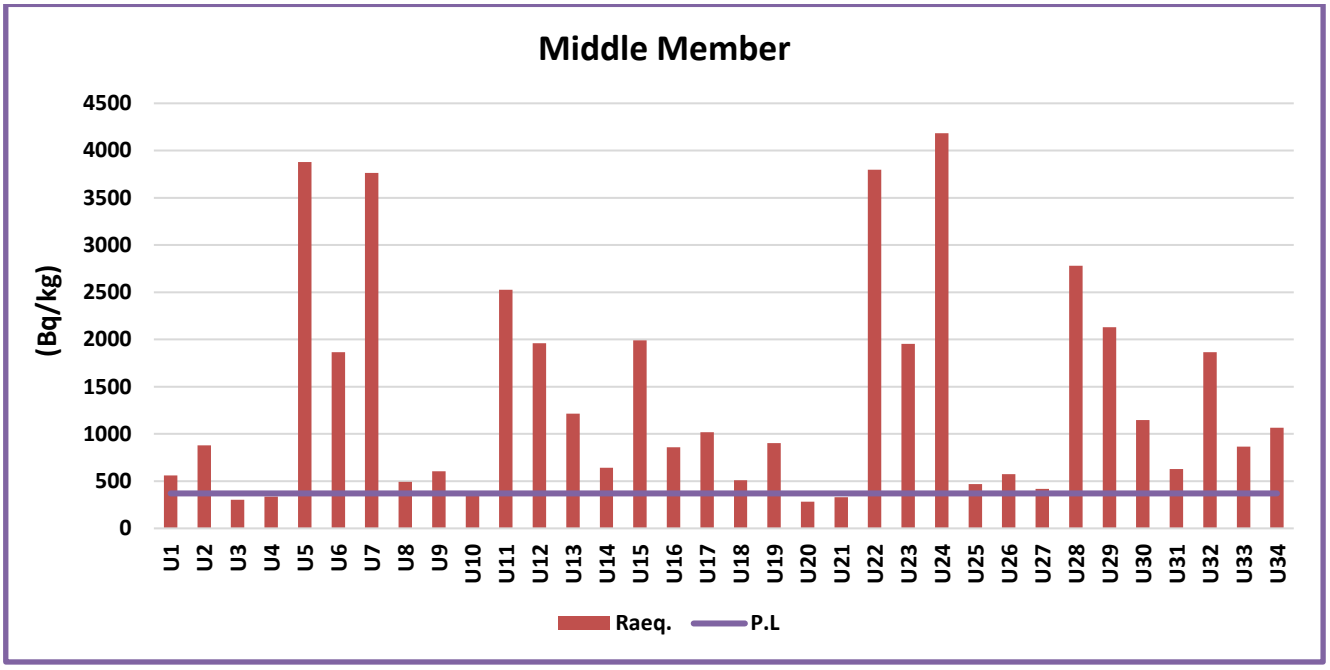

Fig. (5): The radium equivalent for the middle member samples

3.2.5. Alpha Index (I_α)

The alpha index has been proposed to assess the level of exposure due to radon inhalation from building materials using equation (13) [26].

$$I_\alpha = 0.005\, A_{Ra} \quad \leq 1 \qquad \textbf{(13)}$$

The recommended upper level for ^{226}Ra is 200 Bq/kg. The mean alpha index result in the studied area was 4.70, which is greater than the allowable level.

3.2.6. Gamma Index (I_γ)

The gamma emission index, I_γ is one of the health indices that assess the excess external and internal gamma radiation from building materials [26].

$$I_\gamma = \frac{A_{Ra}}{150} + \frac{A_{Th}}{100} + \frac{A_K}{1500} \leq 1 \qquad \textbf{(14)}$$

The average value of gamma index for all samples was 7.66, which exceed the maximum permissible value (unity).

3.2.7. Annual Gonad Equivalent Dose ($AGED$)

An increase in annual gonad equivalent dose has been known to affect the bone tissue, causing destruction of the red cells that are then replaced by white blood cells. This situation results in a blood cancer called leukemia which is fatal. $AGED$ was calculated using equation (15) [27].

$$AGED\ (m\,Sv\,y^{-1}) = 3.09\, A_{Ra} + 4.18 A_{Th} + 0.3144 A_K \qquad \textbf{(15)}$$

The mean value of AGDE was 3513.02 $m\,Sv\,y^{-1}$, which is more than the world limit value (300 $m\,Sv\,y^{-1}$). Consequently, the residents of the study area face a threat to their bone marrow and bone surface.

3.2.8. Excess Lifetime Cancer Risk ($ELCR$)

The excess lifetime cancer risk predicts the chance of contracting cancer over a lifetime at a given level of exposure. The subsequent equation is used to calculate the $ELCR$ [17].

$$ELCR = AEDE_{total}\ x\ DL\ x\ RF \qquad \textbf{(16)}$$

where DL is the average life span (70 years) and RF is the risk factor coefficient (Sv^{-1}). The International Commission on Radiological Protection (ICRP-60) recommendation is RF = 0.057. ELCR was calculated with an average of 12.72, which is much higher than the global average of 0.29×10^{-3}.

Table (4): Descriptive statistics of radiological hazard indices at the studied area

Locality	Lithology		D_{air} (*nGy/h*)	Ra_{eq} (*Bq/kg*)	$AEDE_{out}$ (*m Sv y^{-1}*)	$AEDE_{indoor}$ (*m Sv y^{-1}*)	H_{ex}	H_{in}	I_{α}	I_{γ}	AGED (*m Sv y^{-1}*)	$AEDE_{total}$ (*m Sv y^{-1}*)	ELCR
West Gabal Adediya	Siltstone	Range	43.68 -1934.83	96.44-4182.39	0.05- 2.37	0.21- 9.50	0.26-11.32	0.46 - 21.95	0.37-19.67	0.65-28.15	294.29-12994.44	0.27 -11.87	1.07 - 47.37
		Average	774.80	1672.73	0.95	3.80	4.54	8.54	7.40	11.35	5223.63	4.75	18.97
	Claystone	Range	180.96-907.99	394.69-1945.02	0.22-1.11	0.89-4.46	1.08-5.30	1.58-10.01	0.94-8.71	2.80-13.29	1246.66-6125.74	1.11-5.57	4.43-22.23
		Average	404.16	867.04	0.50	1.98	2.36	4.11	3.23	6.03	2754.01	2.48	9.90
	Shale	Range	153.06-231.06	329.66-493.10	0.19-0.28	0.75-1.13	0.90-1.35	1.31-2.08	0.75-1.35	2.37-3.54	1060.02-1595.82	0.94-1.42	3.75-5.66
		Average	190.00	406.76	0.23	0.93	1.11	1.68	1.04	2.92	1313.65	1.17	4.65
	Dolostone	Range	105.40-129.10	228.13-278.78	0.13-0.16	0.52-0.63	0.62-0.76	1.18-1.45	1.04-1.29	1.54-1.88	708.74-868.15	0.65-0.79	2.58-3.16
		Average	115.89	250.66	0.14	0.57	0.68	1.30	1.15	1.69	779.35	0.71	2.84
	Dolomite	Average	101.45	219.84	0.12	0.50	0.60	1.13	0.99	1.48	682.36	0.62	2.48
	Average		519.34	1119.24	0.64	2.55	3.04	5.58	4.70	7.66	3513.02	3.19	12.72
	P.L		59 [a]	370 [a]	0.7 [a]	0.05 [a]	≤ 1 [a]	≤ 1 [a]	≤ 1 [a]	≤ 1 [a]	300 [b]	-	$0.29x10^{-3}$ [a]

a: [5]; b: [6]

4. CONCLUSIONS AND RECOMMENDATIONS

Radioactivity levels of the environment vary with the geological characteristics of rock samples, where they are found in different concentration. The activity concentrations of the radionuclides ^{238}U, ^{232}Th, and ^{40}K in forty-five sedimentary rock samples collected from three members at southwestern Sinai, Egypt were measured using gamma-ray spectrometry with a high-purity germanium (HPGe) detector. Siltstone has a higher average activity concentration value for ^{238}U, however claystone has a higher value for ^{232}Th and ^{40}K. The contribution of the average activity concentrations of the radionuclides for the studied area are ordered as follows ^{238}U followed by ^{226}Ra, ^{40}K, ^{232}Th then ^{235}U. The study of radionuclides and their creation in natural samples has become one of the most important issues due to its impact on human health, plant, and animal. The obtained results show that the dispersal of radionuclides activity concentrations in the sedimentary sample varieties affects the values of all hazard indices such as absorbed dose rate, radium equivalent, outdoor and indoor annual effective doses, gamma index, alpha index, excess lifetime cancer risk, annual gonad equivalent dose, internal and external hazard indices. All the measured hazards indices were found to be higher than the worldwide limit. The studied area is rather risky for human outdoor activities such as agriculture, construction, and industry. Since the average value of the external hazard index is greater than one, these rocks should not be used for construction for safety reasons.

CONFLICT OF INTEREST STATEMENT:

There is no conflict of interest.

REFERENCES

[1] Saleh M A, Ramli A T, Alajerami Y, Mhareb M H A, Aliyu A S, Gabdo H T and Garba N N (2014) Assessment of radiological health from ambient environment in the Muar district, Johor, Malaysia *Radiation Physics and Chemistry* **103** 243–52

[2] Harb S, Abbady A, El-Kamel A H, Abd El-Mageed A I and Rashed W (2009) Concentration of U-238, U-235, Ra-226, Th-232 And K- 40 for Some Granite Samples in Eastern Desert of Egypt, *Proceedings of the 3rd Environmental Physics Conference (EPC-2008)* p 335

[3] Akpanowo M A, Umaru I, Iyakwari S, Joshua E O, Yusuf S and Ekong G B (2020) Determination of natural radioactivity levels and radiological hazards in environmental samples from artisanal mining sites of Anka, North-West Nigeria, *Scientific African* **10**

[4] Rajesh S and Kerur B (2018) Assessment of natural radioactivity levels due to 238 U, 232 Th, and 40 K in the soil samples of Raichur district, Karnataka, India, *Radiation Protection and Environment* **41** 51

[5] UNSCEAR (2008) Sources and Effects of Ionizing Radiation. United Nations Scientific Committee on the Effects of Atomic Radiation *Report to the General Assembly Scientific Annexes A and B* **1**

[6] UNSCEAR (2000) Source and Effects of Ionizing Radiation. United Nations Scientific Committee on the Effects of Atomic Radiation *Report to General Assembly, Scientific Annexes, United Nations, New York* 265–73

[7] Morsy A M, Hassein H A and El Fki M Y Sedimentology of the Paleozoic in west Central Sinai *Proc. 3rd conf. Geol., Sinai Develop, Ismailia* pp 113-126 (1992)

[8] El Shahat A and Kora M (1988) Composition of the Early Carboniferous dolostones of Um Bogma Formation, *Bulletin of the Faculty of Science, Mansou228University* **15** 33–58

[9] El-Agami N L Geology and radioactivity studies on the Paleozoic rock units in the Sinai Peninsula, Egypt *Ph. D. Thesis, Fac. of Science, Mansoura Univ. Egypt* 302 (1996)

[10] El Aassy I E, El Galy M M, Nada A A, El Feky M G, Abd El Maksoud T M, Talaat S M and Ibrahim E M (2011) Effect of alteration processes on the distribution of radionuclides in uraniferous sedimentary rocks and their environmental impact, southwestern Sinai, Egypt, *Journal of Radioanalytical and Nuclear Chemistry* **289** 173–84

[11] Refaat A Comparative mineralogical and Geochemical studies on the minerlizations in the contact zone between the Adediya and Um Bogma formations in Wadi Um Hamd area, South Western Sinai, Egypt *M.Sc Thesis, Fac. of Sci., Ain Shams Univ., Egypt* 188 (2017)

[12] IAEA (1987) *Preparation and certification of IAEA gamma-ray spectrometry reference materials RGU-1, RGTh-1 and RGK-1. International Atomic Energy Agency*

[13] El Aassy I E, Talaat S M, Abd El Maksoud T M and Zaghloul A M (2017) 238U Radionuclides Radionuclides Series Ratios As A Guide For Alteration Processes Grades And Times of Different Rock Samples, Southwestern Sinai,

Egypt, *International Journal of Engineering Science Invention* **6** 23–34

[14] Papachristodoulou C A, Assimakopoulos P A, Patronis N E and Ioannides K G (2003) Use of HPGe γ-ray spectrometry to assess the isotopic compositiion of uranium in soils, *Journal of Environmental Radioactivity* **64** 195–203

[15] Le T A, Nguyen C T, Bui V L and Lakosi L (2018) Relative efficiency calibration for determining isotopic composition and age of HEU items by passive non-destructive gamma spectrometry, *Applied Radiation and Isotopes* **142** 220–6

[16] Ravisankar R, Chandramohan J, Chandrasekaran A, Prince Prakash Jebakumar J, Vijayalakshmi I, Vijayagopal P and Venkatraman B (2015) Assessments of radioactivity concentration of natural radionuclides and radiological hazard indices in sediment samples from the East coast of Tamilnadu, India with statistical approach, *Marine Pollution Bulletin* **97** 419–30

[17] Tawfic A F, Zakaly H M H, Awad H A, Tantawy H R, Abbasi A, Abed N S and Mostafa M (2021) Natural radioactivity levels and radiological implications in the high natural radiation area of Wadi El Reddah, Egypt, *Journal of Radioanalytical and Nuclear Chemistry* **327** 643–52

[18] Özden S and Aközcan S (2021) Natural radioactivity measurements and evaluation of radiological hazards in sediment of Aliağa Bay, İzmir (Turkey), *Arabian Journal of Geosciences* **14**

[19] El-Taher A, Zakaly H M H and Elsaman R (2018) Environmental implications and spatial distribution of natural radionuclides and heavy metals in sediments from four harbours in the Egyptian Red Sea coast, *Applied Radiation and Isotopes* **131** 13–22

[20] Oyeyemi K D, Usikalu M R, Aizebeokhai A P, Achuka J A and Jonathan O (2017) Measurements of radioactivity levels in part of Ota Southwestern Nigeria: Implications for radiological hazards indices and excess lifetime cancer-risks, *Journal of Physics: Conference Series* **852**

[21] Hannan M, Wahid K and Nguyen N (2015) Assessment of natural and artificial radionuclides in Mission (Texas) surface soils, *Journal of Radioanalytical and Nuclear Chemistry* **305** 573–82

[22] Innocent A J, Onimisi M Y and Jonah S A (2013) Evaluation of Naturally Occurring Radionuclide in Soil Samples from Erena Mining Sites in Niger State, Nigeria, *British Journal of Applied Science and Technology* **4** 684–92

[23] Wang Z, He J, Du Y, He Y, Li Z, Chen Z and Yang C (2011) Natural and artificial radionuclide measurements and radioactivity assessment of soil samples in eastern Sichuan province (China), *Radiation Protection Dosimetry* **150** 391–7

[24] Darwish D A E, Abul-Nasr K T M and El-Khayatt A M (2015) The assessment of natural radioactivity and its associated radiological hazards and dose parameters in granite samples from South Sinai, Egypt, *Journal of Radiation Research and Applied Sciences* **8** 17–25

[25] Adagunodo T A, George A I, Ojoawo I A, Ojesanmi K and Ravisankar R (2018) Radioactivity and radiological hazards from a kaolin mining field in Ifonyintedo, Nigeria, *MethodsX* **5** 362–74

[26] Vishnu C V and Joseph A (2022) Determination of natural radioactivity, hazard parameters and physico-chemical properties of soils from Palakkad-Thrissur district, Kerala, India, *Materials Today: Proceedings*

[27] El-shanshoury G I and Arafat A A (2018) Statistical Analysis of Natural Radioactivity Measurements for the Soil of Marsa Alam-Shalateen Red-Sea Coast Area, Egypt, *International Journal of Advanced Scientific and Technical Research* **1** 71–85